Journal of Organometallic Chemistry, 402 (1991) 85–96
Elsevier Sequoia S.A., Lausanne
JOM 21270

The X-ray crystal structures of $[Mo(C{\equiv}CPh)(Ph_2PCH_2CH_2PPh_2)(\eta\text{-}C_7H_7)]$ and $[Mo(C{\equiv}CPh)(Ph_2PCH_2CH_2PPh_2)(\eta\text{-}C_7H_7)][BF_4]$ (C_7H_7 = cycloheptatrienyl): an investigation of metal–alkynyl bonding

Roy L. Beddoes, Caroline Bitcon and Mark W. Whiteley *
Department of Chemistry, University of Manchester, Manchester M13 9PL (UK)

(Received July 6th, 1990)

Abstract

Single crystal X-ray diffraction studies have been carried out on the cycloheptatrienylmolybdenum alkynyl complexes $[Mo(C{\equiv}CPh)(dppe)(\eta\text{-}C_7H_7)]$ (**1**) and $[Mo(C{\equiv}CPh)(dppe)(\eta\text{-}C_7H_7)][BF_4]$ (**2**-$[BF_4]$) (dppe = $Ph_2PCH_2CH_2PPh_2$) to investigate the structural effects of one-electron oxidation of **1**. The major structural alterations resulting from oxidation of **1** to **2**-$[BF_4]$ are an increase of 0.061(2) Å in the mean Mo–phosphorus separation and a decrease of 0.071(10) Å in the Mo–alkynyl carbon bond length. The mean Mo to cycloheptatrienyl carbon distance and the alkynyl C≡C bond length are virtually unchanged. These observations are consistent with a metal-based redox site in **1** and, in conjunction with the results of electrochemical and infrared studies, suggest that the alkynyl ligand in **1** acts predominantly as a σ-donor to molybdenum with any contribution to the metal–alkynyl bond from a $d\pi$ (metal) $\rightarrow \pi^*$ (alkynyl) interaction being relatively insignificant in this particular example.

The precise description of bonding between a transition metal and alkynyl ligand has been the recurrent focus of a wide range of investigations. Simple symmetry considerations suggest the possibility of π-interaction between filled metal *d* orbitals and alkynyl C≡C-$p\pi^*$ orbitals and the interpretation of some infrared, [1] NMR [2] and Mössbauer [3] studies has given support to this view. Moreover, in practice, a transition metal to alkynyl ligand bond is frequently kinetically more stable than the analogous metal–alkyl bond; an example pertinent to this paper is provided by the relative stability of $[Mo(C{\equiv}CPh)(CO)_2(\eta\text{-}C_7H_7)]$ [4] compared with $[Mo(Me)(CO)_2(\eta\text{-}C_7H_7)]$ [5]. However, much recent work, including theoretical studies on $[Fe(C{\equiv}CH)L_2(\eta\text{-}C_5H_5)]$ (L = CO or PH_3) [6] and X-ray crystallographic comparison of appropriate Ru–L′ bond lengths in $[RuL'(PPh_3)_2(\eta\text{-}C_5H_5)]^z$ ($z = 0$, L′ = C≡CPh [7]; $z = +1$, L′ = CO [7] or C=C(Me)Ph [8]), concludes that in these examples the alkynyl ligand acts essentially as a simple σ-donor in bonding to the transition metal.

We have previously described the synthesis and isolation of the cycloheptatrienylmolybdenum alkynyl complex $[Mo(C{\equiv}CPh)(dppe)(\eta\text{-}C_7H_7)]$ (**1**) and its

0022-328X/91/$03.50

17-electron radical cation [Mo(C≡CPh) (dppe) (η-C_7H_7)][BF_4] **2**-[BF_4] [4] and now present details of the X-ray crystal structures of this redox-related pair of complexes. Crystallographic comparisons of the molecular structures of redox pairs have proved to be an excellent experimental method with which to probe metal–ligand bonding [9,10] and the structural comparison of **1** and **2**-[BF_4] presented here provides a hitherto unexplored approach with which to gain an understanding of the transition-metal to alkynyl bond. The X-ray crystallographic characterisation of **1** and **2**-[BF_4] also furthers a more general series of investigations on the structure of cycloheptatrienyl complexes of the group 6 transition metals. To our knowledge, crystallographically characterised half-sandwich complexes of Cr, Mo or W containing a *heptahapto*-bonded cycloheptatrienyl ligand are limited to just 14 previous examples: [$Mo(CO)_3$(η-C_7H_7)]+ [11], [$MX(CO)_2$(η-C_7H_7)] (M = Mo, X = Br [12], Cl [12], C_6F_5 [13], $SnCl_3$ [14] or TePh [15]; M = W, X = SePh [15]), [Mo($SnPh_{3-x}Cl_x$)$(CO)_2$(η-C_7H_7)] ($x = 2$ or 1) [16], [MoL(acac)(η-C_7H_7)]^z (acac = acetylacetonate; z = +1, L = H_2O [17]; $z = 0$, L = NCS [18]), [MoI(CO)(PN*)(η-C_7H_7)] (PN* = (*S*)(+)-Ph_2PN(Me)CH(Me)(Ph)) [19], [MoCl(dppe)(η-C_7H_7)] · toluene [20] and [MoI_2(thf)(η-C_7H_7)] (thf = tetrahydrofuran) [21]. Furthermore, in the case of [MoCl(dppe)(η-C_7H_7)] · toluene, only a few selected data were reported [20].

Results and discussion

Complexes **1** and **2**-[BF_4] were prepared as described previously [4] and crystal structures determined by room temperature single-crystal X-ray diffraction studies, full details of which are given in the Experimental section. Selected derived bond lengths and angles for **1** and **2**-[BF_4] are listed in Tables 1 and 2. Figures 1 and 2 show the non-hydrogen frameworks of **1** and **2**-[BF_4] respectively together with the atomic labelling scheme adopted; a few minor differences in the atomic labelling of **1** and **2**-[BF_4] are evident and therefore care should be exercised in the direct comparison of individual bond lengths and angles involving the phenyl and cycloheptatrienyl rings. We have recently reported [22] on the very slow dimerisation of the radical cation (**2**) to give divinylidene-bridged [$Mo_2(dppe)_2$(η-C_7H_7)$_2$(μ-C_4Ph_2)]$^{2+}$ via coupling at C_β (C(14)) of the alkynyl ligand of **2**. However the X-ray crystal structure of **2**-[BF_4] exhibits no intermolecular C(14)–C(14) separations shorter than 8.827 Å.

Some general observations about the molecular geometries of **1** and **2**-[BF_4] will be made initially. In each case molybdenum is η^7-bonded to a cycloheptatrienyl ring and further ligated by the alkynyl group and the two phosphorus atoms of the dppe ligand. The C_7H_7 ring in **2**-[BF_4] can be considered as a regular heptagon with C–C bond lengths in the range of 1.362(15)–1.437(16) Å (mean 1.390 Å), internal bond angles in the range 126.2(6)–131.8(8)° (mean 128.6°) and the deviation of carbons from the best ring plane not exceeding ±0.024 Å. By comparison the C_7H_7 ring in **1** appears less regular with C–C bond lengths which extend through the values 1.295(11)–1.469(13) Å (mean 1.371 Å) although internal ring angles lie in the range 125.2(4)–130.6(7)° and deviations of C(6)–C(12) from the best ring plane do not exceed ±0.016 Å. In (**1**), for which the hydrogen atom positions were allowed to refine, the C_7H_7 hydrogens are displaced out of the mean ring plane by an average of 0.08 Å towards molybdenum; this observation is consistent with theoretical studies [23] and other crystallographic work on cycloheptatrienylmolybdenum derivatives [18].

Table 1

Bond lengths (Å) and angles (°) for **1**

Mo(1)-P(2)	2.467(1)	P(5)-C(4)	1.849(5)
Mo(1)-P(5)	2.477(1)	P(5)-C(33)	1.836(5)
Mo(1)-C(13)	2.138(5)	P(5)-C(39)	1.847(5)
Mo(1)-C(6)	2.271(6)	C(13)-C(14)	1.205(6)
Mo(1)-C(7)	2.255(6)	C(14)-C(15)	1.434(7)
Mo(1)-C(8)	2.265(6)	C(6)-C(7)	1.426(13)
Mo(1)-C(9)	2.270(5)	C(7)-C(8)	1.469(13)
Mo(1)-C(10)	2.289(6)	C(8)-C(9)	1.365(12)
Mo(1)-C(11)	2.303(6)	C(9)-C(10)	1.359(11)
Mo(1)-C(12)	2.265(6)	C(10)-C(11)	1.316(10)
P(2)-C(3)	1.841(4)	C(11)-C(12)	1.295(11)
P(2)-C(21)	1.842(5)	C(12)-C(6)	1.367(12)
P(2)-C(27)	1.827(4)		
P(2)-Mo(1)-P(5)	78.2(1)	C(3)-P(2)-C(21)	101.5(2)
C(6)-Mo(1)-C(13)	107.2(4)	C(3)-P(2)-C(27)	104.1(2)
C(7)-Mo(1)-C(13)	86.7(4)	C(21)-P(2)-C(27)	101.6(2)
C(8)-Mo(1)-C(13)	91.7(3)	C(4)-P(5)-C(33)	105.0(2)
C(9)-Mo(1)-C(13)	116.6(2)	C(4)-P(5)-C(39)	101.7(2)
C(10)-Mo(1)-C(13)	150.0(2)	C(33)-P(5)-C(39)	99.2(2)
C(11)-Mo(1)-C(13)	171.0(3)	Mo(1)-C(13)-C(14)	178.5(4)
C(12)-Mo(1)-C(13)	138.9(2)	C(13)-C(14)-C(15)	177.9(5)
C(13)-Mo(1)-P(2)	77.3(2)	C(6)-C(7)-C(8)	125.2(4)
C(13)-Mo(1)-P(5)	83.8(2)	C(7)-C(8)-C(9)	126.2(4)
Mo(1)-P(2)-C(3)	108.1(1)	C(8)-C(9)-C(10)	129.9(4)
Mo(1)-P(2)-C(21)	119.9(2)	C(9)-C(10)-C(11)	129.7(4)
Mo(1)-P(2)-C(27)	119.2(2)	C(10)-C(11)-C(12)	130.6(4)
Mo(1)-P(5)-C(4)	111.2(2)	C(11)-C(12)-C(6)	130.6(7)
Mo(1)-P(5)-C(33)P	117.0(2)	C(12)-C(6)-C(7)	127.8(7)
Mo(1)-P(5)-C(39)	120.7(2)		

A number of modifications in the geometry of the $[\mathrm{Mo(C{\equiv}CPh)(dppe)}(\eta\text{-}\mathrm{C_7H_7})]$ unit become evident by comparison of **1** and **2**-$[\mathrm{BF_4}]$. In terms of bond lengths the one-electron oxidation of **1** to **2**-$[\mathrm{BF_4}]$ appears to have very little effect upon Mo–$\mathrm{C_7H_7}$ bonding. The molybdenum to $\mathrm{C_7H_7}$ ring plane distances of 1.63 and 1.62 Å in **1** and **2**-$[\mathrm{BF_4}]$ respectively and the mean Mo to C(ring) distances (2.274 Å in **1** and 2.280 Å in **2**-$[\mathrm{BF_4}]$) are almost unchanged. However, consideration of the ring centroid (chtyl)–metal–ligand angles ((chtyl)–Mo–C(13) 131.5°, (chtyl)–Mo–P(2) 133.6°, (chtyl)–Mo–P(5) 131.6° in **1** and (chtyl)–Mo–C(13) 130.6°, (chtyl)–Mo–P(2) 136.1°, (chtyl)–Mo–P(5) 131.5° in **2**-$[\mathrm{BF_4}]$) reveals a small movement of the $\mathrm{C_7H_7}$ ring away from one phosphorus as a result of one-electron oxidation. A further change involves a small additional pyramidalisation of the angles between the tripodal ligand donor atoms. Thus, the sum of P–Mo–P and P–Mo–C(13) angles decreases from 239.3(3)° in **1** to 237.0(4)° in **2**-$[\mathrm{BF_4}]$; a similar effect has been noted for the redox pairs $[\mathrm{Fe(CO)\{P(OMe)_3\}_2}(\eta^4\text{-}\mathrm{C_4Ph_4})]^z$ ($z = 0$ or $+1$) and $[\mathrm{Mn(CO)(dppe)}(\eta^5\text{-}\mathrm{C_6H_6Ph})]^z$ ($z = 0$ or $+1$) [24]. A supplementary point is that the angle summation of 237.0(4)° in **2**-$[\mathrm{BF_4}]$ is smaller than corresponding summations in any previously reported structures of half-sandwich cycloheptatrienylmolybdenum complexes.

Table 2

Bond lengths (Å) and angles (°) for **2**-[BF_4]

Mo(1)-P(2)	2.538(2)	P(5)-C(4)	1.837(8)
Mo(1)-P(5)	2.528(3)	P(5)-C(33)	1.804(9)
Mo(1)-C(13)	2.067(9)	P(5)-C(39)	1.824(10)
Mo(1)-C(6)	2.268(11)	C(13)-C(14)	1.196(11)
Mo(1)-C(7)	2.301(10)	C(14)-C(15)	1.445(12)
Mo(1)-C(8)	2.276(9)	C(6)-C(7)	1.364(14)
Mo(1)-C(9)	2.283(9)	C(7)-C(8)	1.437(16)
Mo(1)-C(10)	2.251(9)	C(8)-C(9)	1.406(15)
Mo(1)-C(11)	2.282(9)	C(9)-C(10)	1.395(16)
Mo(1)-C(12)	2.301(10)	C(10)-C(11)	1.400(16)
P(2)-C(3)	1.820(9)	C(11)-C(12)	1.363(15)
P(2)-C(21)	1.850(9)	C(12)-C(6)	1.362(15)
P(2)-C(27)	1.793(9)		
P(2)-Mo(1)-P(5)	78.4(1)	C(3)-P(2)-C(21)	103.0(3)
C(6)-Mo(1)-C(13)	122.7(4)	C(3)-P(2)-C(27)	105.5(4)
C(7)-Mo(1)-C(13)	96.0(4)	C(21)-P(2)-C(27)	102.0(4)
C(8)-Mo(1)-C(13)	86.1(4)	C(4)-P(5)-C(33)	103.8(3)
C(9)-Mo(1)-C(13)	99.2(4)	C(4)-P(5)-C(39)	105.5(4)
C(10)-Mo(1)-C(13)	128.8(4)	C(33)-P(5)-C(39)	101.8(5)
C(11)-Mo(1)-C(13)	164.8(4)	Mo(1)-C(13)-C(14)	174.6(8)
C(12)-Mo(1)-C(13)	156.8(4)	C(130-C(14)-C(15)	175.0(10)
C(13)-Mo(1)-P(2)	75.1(3)	C(6)-C(7)-C(8)	126.4(6)
C(13)-Mo(1)-P(5)	83.5(3)	C(7)-C(8)-C(9)	129.4(6)
Mo(1)-P(2)-C(3)	106.5(3)	C(8)-C(9)-C(10)	126.2(6)
Mo(1)-P(2)-C(21)	121.6(3)	C(9)-C(10)-C(11)	129.1(6)
Mo(1)-P(2)-C(27)	116.5(3)	C(10)-C(11)-C(12)	129.4(6)
Mo(1)-P(5)-C(4)	109.1(3)	C(11)-C(12)-C(6)	128.3(8)
Mo(1)-P(5)-C(33)	116.4(4)	C(12)-C(6)-C(7)	131.1(8)
Mo(1)-P(5)-C(39)	118.7(4)		

The major changes in molecular geometry between **1** and **2**-[BF_4] involve the molybdenum to phosphorus and molybdenum to alkynyl-carbon bond lengths, Mo-P(2), Mo-P(5) and Mo-C(13). In **1** Mo-P(2) and Mo-P(5) (2.467(1) and 2.477(1) Å) are slightly shorter than the corresponding bond lengths quoted for $[MoCl(dppe)(\eta\text{-}C_7H_7)]\cdot$ toluene (2.50 and 2.49 Å) [20] but one-electron oxidation of **1** results in an increase in the average Mo-phosphorus distance by 0.061(2) Å accompanied by a decrease in the mean phosphorus to phenyl carbon distance from 1.838(5) to 1.818(9) Å and the mean phosphorus to methylene carbon distance from 1.845(5) to 1.829(9) Å. These redox induced modifications in the bond lengths pertaining to the dppe ligand correlate well with extensive data available from structural studies on redox related pairs of metal phosphine complexes in which one-electron oxidation is metal based [9]. Oxidation at the metal centre is accompanied by a decrease in the ability of the metal to act as a π-donor and therefore bonds to ligands with a strong π-acceptor capacity should be weakened and lengthened. The increase in the mean Mo-phosphorus distance by 0.061(2) Å on oxidation of **1** to **2**-[BF_4] is consistent with the π-acceptor properties of the dppe ligand and lies in the mid range of the observed increases in metal-phosphorus bond distances initiated by a metal-based one-electron oxidation [9].

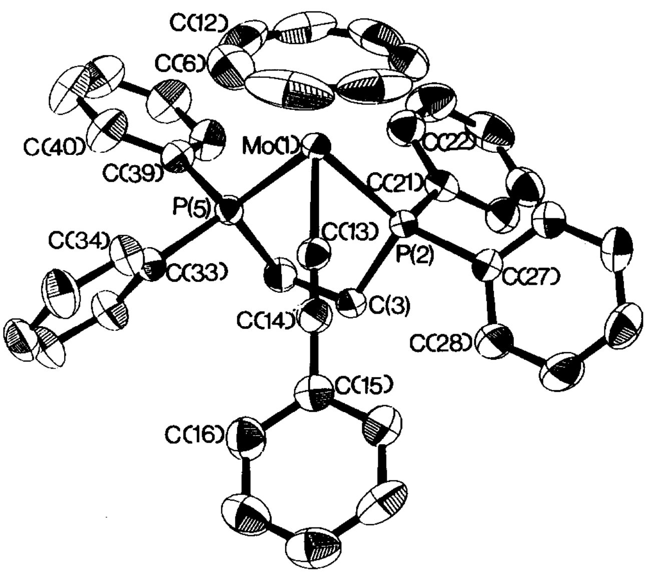

Fig. 1. ORTEP plot of the molecular structure of **1** showing atomic labelling scheme; hydrogen atoms are omitted.

The final part of the discussion concerns the metal–alkynyl interaction. A comparison of structural data for **1** and $[\mathrm{W(C{\equiv}CC_3H_5)(CO)_2(PMe_3)(\eta\text{-}C_5H_5)}]$ [25] reveals almost identical metal to alkynyl carbon and alkynyl C≡C bonds lengths.

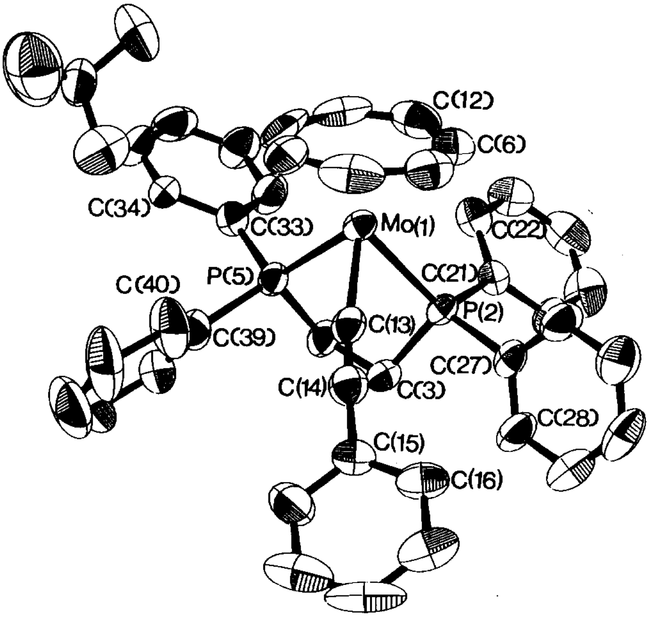

Fig. 2. ORTEP plot of the structure of **2**-$[BF_4]$ showing atomic labelling scheme; hydrogen atoms are omitted.

However, *trans*-[Mo(C≡CPh)$_2$(dppe)$_2$], the only previous example of a crystallographically characterised molybdenum alkynyl complex [26], exhibits a shorter molybdenum to alkynyl–carbon bond length (2.093(8) Å) and longer alkynyl C≡C distance (1.237(12) Å) when compared with **1**. The one-electron oxidation of **1** to **2**-[BF$_4$] gives rise to a decrease in the molybdenum alkynyl bond length Mo–C(13) of 0.071(10) Å (from 2.138(5) Å in **1** to 2.067(9) Å in **2**-[BF$_4$]) but the alkynyl C≡C distance C(13)–C(14) is essentially invariant. In view of the changes in molybdenum to phosphorus bond lengths on formation of **2**-[BF$_4$] from **1** and other data from electrochemical and ESR studies [4], the one-electron oxidation of **1** can be considered to first order to be at molybdenum such that the formal oxidation state increases from Mo^0 in **1** to Mo^I in **2**-[BF$_4$] (assuming that the C$_7$H$_7$ ring bears a unipositive charge). Consequently the radius of the molybdenum atom will decrease and this effect, together with the increased formal charge at molybdenum, should be observed as a tendency for metal–ligand bond lengths to decrease. However any such decrease in metal–ligand bond distances may be moderated or even reversed if the metal–ligand bond involves substantial metal to ligand π back-donation and therefore the net change in bond length reflects a balance between opposing factors. In fact molybdenum to phosphorus bond lengths increase on one-electron oxidation of **1** but, as discussed, this observation is fully consistent with the ability of dppe to acts as a good π-acceptor ligand. The contrasting decrease in the Mo–C(13) bond length brought about by one-electron oxidation of **1** therefore indicates that any $d\pi$ (metal) → π^* (alkynyl) interaction is relatively insignificant since, within the same molecule, the redox induced change in the metal–alkynyl distance is in the opposite sense yet of comparable magnitude to the corresponding change in the metal–phosphorus bond length for the established π-acceptor ligand dppe. A closely related result hs been obtained via one-electron oxidation of *trans*-[TcCl$_2$(dppe)$_2$] to its monocation [27]; in this example one-electron oxidation effects an increase in the average Tc–phosphorus bond length from 2.429(1) to 2.501(1) Å but a decrease in the average Tc–Cl distance from 2.424(1) to 2.319(1) Å in accord with simple σ bonding between technetium and the chloride ligands. Our conclusion that the alkynyl group in **1** acts predominantly as a simple σ-donor ligand is further supported by the effective invariance in the C(13)–C(14) C≡C bond length since, although triple bond lengths are relatively insensitive to small changes in bond order, good π-acceptor ligands such as CO do exhibit a noticeable decrease in the length of the triple bond following electron removal from the metal-based HOMO of complexes such as [Mn(CO)(dppe)(η^5-C$_6$H$_6$Ph)] [28]. A final feature of note in the metal–alkynyl fragment is a small bending away from linearity resulting from one-electron oxidation; the Mo–C(13)–C(14) and C(13)–C(14)–C(15) angles of 178.5(4) and 177.9(5)° respectively in **1** attain corresponding values of 174.6(8) and 175.0(10)° in **2**-[BF$_4$].

The results of this crystallographic investigation tend to exclude any significant π-contribution to metal–alkynyl bonding in **1** but considerable caution should be exercised in the general application of this conclusion. Theoretical studies on [Fe(C≡CH)L$_2$(η-C$_5$H$_5$)] (L = CO or PH$_3$) indicate that a major constraint to $d\pi$ (metal) → π^* (alkynyl) electron transfer is a poor energy match between the relevant donor and acceptor orbitals [6]; however this might be modified via variables such as the metal, its oxidation state and the alkynyl substituent. In principle the extent of $d\pi$ (metal) → π^* (alkynyl) interaction should be increased in alkynyl complexes of metals in a low oxidation state located at the right hand side of the periodic table and very recently the results of spectroscopic and electrochemical studies have been cited as evidence for significant π back-donation from Rh to the alkynyl ligand in the complexes $[Rh(C{\equiv}CR)\{E(CH_2CH_2PPh_2)_3\}]$ (R = Ph or CO_2Et; E = N or P) [29]. However corresponding investigations involving **1** and **2**-$[BF_4]$ do not detract from the conclusions of our crystallographic work.

The electrochemical studies involve the determination of $E°$ values for reversible one-electron oxidation processes in the series of complexes $[RhX\{E(CH_2CH_2PPh_2)_3\}]$ (X = Cl, $C{\equiv}CCO_2Et$, C≡CPh or CN; E = N or P) [29] and $[MoX(dppe)(\eta\text{-}C_7H_7)]$ (X = Cl, C≡CPh or CN) [4,30]. In these complexes variation of the ligand X, whilst maintaining all other factors constant, produces a modification in electron density at the metal centre governed by the combined σ-donor and π-acceptor properties of X. Provided that the one-electron oxidation process is based at the metal centre then $E°$ values will shift to positive potential as electron density at the metal is decreased. If ligands X are arranged in a series of $E°$ increasing to positive potential then the ordering will reflect the relative abilities of the various X ligands to remove electron density from the metal centre; thus ligands to the right of such a series may be considered to possess comparatively good π-acceptor (or conversely poor σ-donor) properties. For example $E°$ values for one-electron oxidation of $[RhX\{N(CH_2CH_2PPh_2)_3\}]$ lie in the order X = Cl ($E° = -0.47$ V) < X = C≡CPh ($E° = -0.45$ V) < X = $C{\equiv}CCO_2Et$ ($E° = -0.26$ V) < X = CN ($E° = -0.19$ V) ($E°$ values vs. SCE determined by cyclic voltammetry in CH_2Cl_2) and the intermediate position of the alkynyl ligands may be taken as evidence that they have some π-acceptor capability relative to Cl (which is very unlikely to function as a π-acceptor ligand) but are less effective π-acceptor ligands than CN [29]. If this interpretation has any general validity then the changed ordering of these ligands in the $E°$ series determined for the one-electron oxidation of $[MoX(dppe)(\eta\text{-}C_7H_7)]$(X = C≡CPh ($E° = -0.15$ V) < X = Cl, ($E° = -0.05$ V) < X = CN ($E° = +0.21$ V) values vs. SCE determined by cyclic voltammetry under the conditions given in ref. 4) suggests that, in **1**, σ donation from C≡CPh to Mo is the most significant component of the metal–alkynyl bond.

Infrared spectroscopy has also been employed as a probe for metal alkynyl bonding. Determination of the alkynyl ligand $\nu(C{\equiv}C)$ stretching frequency in the complexes $[Rh(C{\equiv}CR)\{E(CH_2CH_2PPh_2)_3\}]^z$ (R = Ph or CO_2Et; E = N or P; $z = 0$, $+1$ or $+2$) revealed an increase of ca. 30 cm^{-1} in $\nu(C{\equiv}C)$ on oxidation of the Rh^I ($z = 0$) complexes to the Rh^{II} ($z = +1$) species and a further increase of ca. 10 cm^{-1} on formation of the Rh^{III} ($z = +2$) derivatives. These changes in $\nu(C{\equiv}C)$ are thought to be consistent with the alkynyl ligand acting as a π-acceptor since oxidation at the metal centre should reduce electron density available for any Rh $d\pi \rightarrow \pi^*$ (alkynyl) interaction and depopulation of the alkynyl π^* orbitals would lead to a strengthening of the C≡C bond [29]. By contrast oxidation of **1** to **2**-$[BF_4]$ effects a decrease in $\nu(C{\equiv}C)$ by 13 cm^{-1} [4] and this result is inconsistent with the operation of significant $d\pi$ (metal) $\rightarrow \pi^*$ (alkynyl) bonding in **1**.

Conclusion

The reversible one-electron oxidation of **1** to its isolable radical cation **2**-$[BF_4]$ has facilitated an investigation of metal–alkynyl bonding by crystallographic and spectroscopic methods; the results suggest that σ donation from C≡CPh to Mo is the major component of metal–alkynyl bonding in **1**. There is no evidence to support any significant $d\pi$ (metal) → π^* (alkynyl) interaction in these complexes but the operation of a small π component cannot be totally excluded since the probe techniques determine net changes resulting from the opposing but combined effects of σ-donor and π-acceptor properties.

Experimental

The majority of details of the structure analyses carried out on **1** and **2**-[BF_4] are given in Table 3; non-hydrogen atom positional parameters for **1** and **2**-[BF_4] are

Table 3

Structure Analyses

	1	**2**-[BF_4]
Crystal data		
Formula	$C_{41}C_{36}MoP_2$	$C_{41}H_{36}BF_4MoP_2$
M	686.6	773.4
Crystal system	triclinic	monoclinic
Space group	$P\bar{1}$ (No. 2)	$P2_1/c$ (No. 14)
a (Å)	9.540(6)	10.412(2)
b (Å)	10.063(3)	15.104(1)
c (Å)	18.608(3)	22.981(2)
α (°)	81.14(2)	90
β (°)	81.17(4)	97.90(2)
γ (°)	69.80(4)	90
U (Å^3)	1646.8	3579.8
T (K)	294	294
Z	2	4
D_c (g cm^{-3})	1.38	1.43
F(000)	708	1580
μ(Mo-K_α) (cm^{-1})	5.6	5.4
Data collection reduction		
Crystal dimension (mm)	0.10 × 0.19 × 0.21	0.06 × 0.09 × 0.20
Wavelength (Å) (graphite monochromated Mo-K_α)	0.71069	0.71069
θ-range (°)	1–25	1–25
Scan mode	$\omega/2\theta$	$\omega/2\theta$
Scan width	$(0.90 + 0.35 \tan\theta)$	$(0.5 + 0.35 \tan\theta)$
Total data	5857	5520
Unique data	5857	5520
'Observed' data (NO)	4160	2767
Observation criterion ($F > n\sigma(F)$)	3	3
Refinement		
Least squares variables (NV)	542	443
R [a]	0.0433	0.0599
R_w	0.0471	0.0553
S	0.959	0.970
w	$1/(4.2 - 0.17F + 0.0027F^2)^{1/2}$	$1/(31.62 - 0.79F + 0.0043F^2)^{1/2}$
Difference map features (eÅ^{-3})	+0.5, −0.2	+0.5, −0.4

[a] $R = \Sigma|\Delta|/\Sigma|F_o|$; $R_w = [\Sigma w\Delta^2/\Sigma wF_o^2]^{1/2}$; $S = \Sigma w\Delta^2/(NO - NV)]^{1/2}$; $\Delta = F_o - F_c$.

Table 4

Atomic coordinates for **1**

Atom	*x*	*y*	*z*
Mo(1)	0.13745(5)	0.38335(4)	0.19614(2)
P(2)	0.1358(1)	0.6306(1)	0.1896(1)
C(3)	0.1190(5)	0.6745(5)	0.2837(2)
C(4)	0.2375(6)	0.5580(5)	0.3246(2)
P(5)	0.2370(1)	0.3794(1)	0.3121(1)
C(6)	0.1599(14)	0.1503(7)	0.2000(4)
C(7)	0.0292(10)	0.2358(12)	0.1659(6)
C(8)	0.0247(8)	0.3491(10)	0.1053(5)
C(9)	0.1427(11)	0.3922(7)	0.0732(3)
C(10)	0.2880(9)	0.3440(8)	0.0880(4)
C(11)	0.3548(7)	0.2412(8)	0.1367(5)
C(12)	0.3010(10)	0.1603(7)	0.1859(4)
C(13)	−0.0746(5)	0.4862(5)	0.2545(2)
C(14)	−0.1937(5)	0.5471(5)	0.2869(3)
C(15)	−0.3325(5)	0.6217(5)	0.3270(3)
C(16)	−0.3618(6)	0.5865(6)	0.4019(3)
C(17)	−0.4909(7)	0.6619(7)	0.4409(3)
C(18)	−0.5983(7)	0.7714(7)	0.4076(4)
C(19)	−0.5749(6)	0.8052(6)	0.3333(4)
C(20)	−0.4448(6)	0.7319(5)	0.2932(3)
C(21)	0.3030(5)	0.6770(5)	0.1477(2)
C(22)	0.4411(6)	0.5694(6)	0.1418(3)
C(23)	0.5695(7)	0.6018(7)	0.1135(4)
C(24)	0.5631(7)	0.7391(7)	0.0906(3)
C(25)	0.4279(7)	0.8455(6)	0.0959(3)
C(26)	0.2990(6)	0.8166(5)	0.1244(3)
C(27)	−0.0145(5)	0.7752(5)	0.1477(2)
C(28)	−0.1278(6)	0.8698(6)	0.1882(3)
C(29)	−0.2367(7)	0.9815(7)	0.1534(3)
C(30)	−0.2340(6)	0.9982(6)	0.0788(3)
C(31)	−0.1224(7)	0.9040(6)	0.0387(3)
C(32)	−0.0142(6)	0.7931(5)	0.0727(3)
C(33)	0.1369(5)	0.3224(5)	0.3970(2)
C(34)	0.0382(6)	0.2507(5)	0.3950(3)
C(35)	−0.0279(6)	0.1986(6)	0.4501(3)
C(36)	0.0035(6)	0.2179(6)	0.5260(3)
C(37)	0.1009(7)	0.2898(6)	0.5282(3)
C(38)	0.1671(6)	0.3416(6)	0.4644(3)
C(39)	0.4311(5)	0.2676(5)	0.3282(2)
C(40)	0.4585(6)	0.1291(6)	0.3619(3)
C(41)	0.6030(7)	0.0416(6)	0.3722(4)
C(42)	0.7213(6)	0.0903(6)	0.3516(4)
C(43)	0.6968(6)	0.2270(6)	0.3181(4)
C(44)	0.5525(6)	0.3146(6)	0.3061(3)

listed in Tables 4 and 5 respectively. X-ray diffraction measurements were made on single crystals using an Enraf Nonius CAD4 diffractometer system. Brown crystals of **1** were obtained from dichloromethane–diethyl ether solution at 0 °C and burgundy-red prismatic crystals of **2**-[BF_4] were grown at the interface of a dichloromethane–diethyl ether layer at room temperature. Cell dimensions were determined

Table 5

Atomic coordinates for **2**-[BF_4]

Atom	x	y	z
Mo(1)	−0.22241(1)	0.09995(1)	0.11843(1)
P(2)	−0.2445(2)	0.1622(2)	0.2192(1)
C(3)	−0.2715(8)	0.2807(6)	0.2094(4)
C(4)	−0.3818(9)	0.2953(6)	0.1598(4)
P(5)	−0.3494(2)	0.2403(2)	0.0920(1)
C(6)	−0.2161(12)	−0.0420(7)	0.1510(5)
C(7)	−0.1009(10)	−0.0276(7)	0.1305(5)
C(8)	−0.0836(10)	0.0129(7)	0.0756(6)
C(9)	−0.1770(14)	0.0457(7)	0.0308(4)
C(10)	−0.3109(12)	0.0455(8)	0.0309(4)
C(11)	−0.3827(10)	0.0110(8)	0.0729(6)
C(12)	−0.3405(12)	−0.0274(7)	0.1257(5)
C(13)	−0.0681(9)	0.1862(6)	0.1371(4)
C(14)	0.0225(10)	0.2332(7)	0.1525(4)
C(15)	0.1376(9)	0.2834(6)	0.1737(4)
C(16)	0.2184(9)	0.2554(7)	0.2221(5)
C(17)	0.3260(10)	0.3031(9)	0.2421(5)
C(18)	0.3555(11)	0.3802(9)	0.2152(7)
C(19)	0.2786(13)	0.4065(9)	0.1679(7)
C(20)	0.1679(11)	0.3609(7)	0.1466(5)
C(21)	−0.3776(8)	0.1277(5)	0.2597(4)
C(22)	−0.4894(8)	0.0898(6)	0.2305(4)
C(23)	−0.5902(9)	0.0663(7)	0.2616(5)
C(24)	−0.5792(10)	0.0786(7)	0.3215(5)
C(25)	−0.4720(11)	0.1174(8)	0.3500(4)
C(26)	−0.3703(9)	0.1433(6)	0.3201(4)
C(27)	−0.1055(8)	0.1522(6)	0.2742(3)
C(28)	−0.0524(10)	0.2230(7)	0.3055(4)
C(29)	0.0468(11)	0.2147(8)	0.3485(4)
C(30)	0.0969(10)	0.1333(9)	0.3630(4)
C(31)	0.0484(11)	0.0615(8)	0.3321(5)
C(32)	−0.0519(10)	0.0693(7)	0.2874(4)
C(33)	−0.5082(9)	0.2271(6)	0.0504(4)
C(34)	−0.5247(9)	0.2351(6)	−0.0102(4)
C(35)	−0.6404(12)	0.2210(8)	−0.0421(4)
C(36)	−0.7470(10)	0.1981(7)	−0.0142(5)
C(37)	−0.7327(9)	0.1885(8)	0.0448(4)
C(38)	−0.6161(10)	0.2023(7)	0.0777(4)
C(39)	−0.2783(9)	0.3252(7)	0.0499(4)
C(40)	−0.1717(11)	0.3068(9)	0.0208(5)
C(41)	−0.1291(13)	0.3715(11)	−0.0147(6)
C(42)	−0.1745(15)	0.4540(12)	−0.0171(7)
C(43)	−0.2795(16)	0.4747(9)	0.0111(6)
C(44)	−0.3290(11)	0.4099(8)	0.0457(4)
B(45)	−0.2859(18)	0.0932(14)	−0.1356(6)
F(46)	−0.3123(8)	0.0127(5)	−0.1131(3)
F(47)	−0.2009(7)	0.0778(6)	−0.1788(4)
F(48)	−0.3896(8)	0.1265(6)	−0.1676(4)
F(49)	−0.2230(13)	0.1456(7)	−0.0971(4)

from the setting angles θ of 25 reflections between 11 and 11.5° for **1** and between 4 and 11° for **2**-$[BF_4]$.

No absorption or extinction corrections were made; in each case no significant intensity drift was observed for standard reflections throughout data collection. The structures were solved by heavy-atom (Patterson and Fourier) methods and refined by least-squares. All non-hydrogen atoms were assigned anisotropic displacement parameters. Hydrogen atoms were introduced at calculated positions and allowed positional and isotropic thermal refinement in **1** but not in **2**-$[BF_4]$ for which hydrogen atom parameters were recalculated as the structure converged. Complex neutral atom scattering factors were taken from ref. 31 and, with the exception of ORTEP [32], all calculations were carried out with programs designed by Mr. O.S. Mills.

Acknowledgements

We are grateful to the S.E.R.C. for the award of a Research Studentship to (C.B.) and to Mr. O.S. Mills for the design and provision of software required for the solution of the crystal structures.

References

1 H. Masai, K. Sonogashira and N. Hagihara, J. Organomet. Chem., 26 (1970) 271.
2 G.W. Parshall, J. Am. Chem. Soc., 88 (1966) 704.
3 T. Birchall and R.D. Myers, Spectrosc. Int. J., 2 (1983) 22.
4 J.S. Adams, C. Bitcon, J.R. Brown, D. Collison, M. Cunningham and M.W. Whiteley, J. Chem. Soc., Dalton Trans, (1987) 3049.
5 W.H. Dell and and M.L. Ziegler, Z. Naturforsch., B, 37 (1982) 1.
6 N.M. Kostic and R.F. Fenske, Organometallics, 1 (1982) 974.
7 J.M. Wisner, T.J. Bartczac and J.A. Ibers, Inorg. Chim. Acta, 100 (1985) 115.
8 M.I. Bruce, M.G. Humphrey, M.R. Snow, and E.R.T. Tiekink, J. Organomet. Chem., 314 (1986) 213.
9 A.G. Orpen and N.G. Connelly, Organometallics, 9 (1990) 1206.
10 R.P. Aggarwal, N.G. Connelly, M.C. Crespo, B.J. Dunne, P.M. Hopkins and A.G. Orpen, J. Chem. Soc., Chem. Commun., (1989) 33.
11 G.R. Clark and G.J. Palenik, J. Organomet. Chem., 50 (1973) 185.
12 M.L. Ziegler, H.E. Sasse and B. Nuber, Z. Naturforsch., B, 30 (1975) 26.
13 M.R. Churchill and T.A. O'Brien, J. Chem. Soc., A, (1969) 1110.
14 M.L. Ziegler, H.E. Sasse and B. Nuber, Z. Naturforsch., B, 30 (1975) 22.
15 A. Rettenmeier, K. Weidenhammmer and M.L. Ziegler, Z. Anorg. Allg. Chem., 473 (1981) 91.
16 H.E. Sasse and M.L. Ziegler, Z. Anorg. Allg. Chem., 402 (1973) 129.
17 M. Green, H.P. Kirsch, F.G.A. Stone and A.J. Welch, J. Chem. Soc., Dalton Trans., (1977) 1755.
18 M. Green, H.P. Kirsch, F.G.A. Stone and A.J. Welch, Inorg. Chim. Acta, 29 (1978) 101.
19 H. Brunner, M. Muschiol, I. Bernal and G.M. Reisner, J. Organomet. Chem., 198 (1980) 169.
20 M.L.H. Green and R.B.A. Pardy, Polyhedron, 4 (1985) 1035.
21 A. Gourdon and K. Prout, Acta Crystallogr., Sect. B, 38 (1982) 1596.
22 R.L. Beddoes, C. Bitcon, A. Ricalton and M.W. Whiteley, J. Organomet. Chem., 367 (1989) C21.
23 M. Elian, M.M.L. Chen, D.M.P. Mingos and R. Hoffmann, Inorg. Chem., 15 (1976) 1148.
24 A.G. Orpen, N.G. Connelly, M.W. Whiteley and P. Woodward, J. Chem. Soc., Dalton Trans., (1989) 1751.
25 W. Sieber, M. Wolfgruber, D. Neugebauer, O. Orama and F.R. Kreissl, Z. Naturforsch., B, 38 (1983) 67.
26 N.A. Buang, D.L. Hughes, N. Kashef, R.L. Richards and A.J.L. Pombeiro, J. Organomet. Chem., 323 (1987) C47.

27 K. Libson, M.N. Doyle, R.W. Thomas, T. Nelesnik, M. Woods, J.C. Sullivan, R.C. Elder and E. Deutsch, Inorg. Chem., 27 (1988) 3614.

28 N.G. Connelly, M.J. Freeman, A.G. Orpen, A.R. Sheehan, J.B. Sheridan and D.A. Sweigart, J. Chem. Soc., Dalton Trans., (1985) 1019.

29 C. Bianchini, A. Meli, M. Peruzzini, A. Vacca, F. Laschi, P. Zanello and F.M. Ottaviani, Organometallics, 9 (1990) 360.

30 A. Ricalton and M.W. Whiteley, unpublished results.

31 International Tables for X-ray Crystallography, Vol. IV, Kynoch Press Birmingham, 1974.

32 C.K. Johnson, Report ORNL 5138, Oak Ridge, Tennessee, 1976.